An RGD Spacing of 440 nm Is Sufficient for Integrin $\alpha_v\beta_3$-mediated Fibroblast Spreading and 140 nm for Focal Contact and Stress Fiber Formation

Stephen P. Massia* and Jeffrey A. Hubbell

Department of Chemical Engineering and * Division of Biological Sciences, University of Texas at Austin, Austin, Texas 78712-1062

Abstract. The synthetic peptide Gly-Arg-Gly-Asp-Tyr (GRGDY), which contains the RGD sequence of several adhesion molecules, was covalently grafted to the surface of otherwise poorly adhesive glass substrates and was used to determine the minimal number of ligand–receptor interactions required for complete spreading of human foreskin fibroblasts. Well-defined adhesion substrates were prepared with GRGDY between 10^{-3} fmol/cm^2 and 10^4 fmol/cm^2. As the adhesion ligand surface concentration was varied, several distinct morphologies of adherent cells were observed and categorized. The population of fully spread cells at 4 h reached a maximum at 1 fmol/cm^2, with no further increases up to 10^4 fmol/cm^2. Although maximal cell spreading was obtained at 1 fmol/cm^2, focal contacts and stress fibers failed to form at RGD surface concentrations below 10 fmol/cm^2. The minimal peptide spacings obtained in this work correspond to 440 nm for spreading and 140 nm for focal contact formation, and are much larger than those reported in previous studies with adsorbed adhesion proteins, adsorbed RGD–albumin conjugates, or peptide-grafted polyacrylamide gels. Vitronectin receptor antiserum specific for integrin $\alpha_v\beta_3$ blocked cell adhesion and spreading on substrates containing 100 fmol/cm^2 of surface-bound GRGDY, while fibronectin receptor antiserum specific for $\alpha_5\beta_1$ did not. Furthermore, $\alpha_v\beta_3$ was observed to cluster into focal contacts in spread cells, but $\alpha_5\beta_1$ did not. It was thus concluded that a peptide-to-peptide spacing of 440 nm was required for $\alpha_v\beta_3$-mediated cellular spreading, while 140 nm was required for $\alpha_v\beta_3$-mediated focal contact formation and normal stress fiber organization in human foreskin fibroblasts; these spacings represent much fewer ligands than were previously thought to be required.

THE adhesive interaction of cells with extracellular matrix components plays an important role in many cellular functions such as regulation of cell morphology, growth, differentiation, and motility. In recent years, many aspects of the molecular basis of cell adhesion have been elucidated. Adhesion-promoting extracellular matrix proteins such as fibronectin (FN)[1], laminin (LN), and vitronectin (VN) are complex multifunctional molecules which interact with other matrix components and with cell surface receptors. The adhesive signal Arg-Gly-Asp (RGD), located within many cell adhesion proteins, and the integrin class of cell surface adhesion receptors, which recognize this signal, comprise the most universal and well understood adhesion receptor–ligand system (1, 4, 13, 15, 18, 22–24). Several basic questions remain unresolved regarding the interactions of cell adhesion proteins with the integrin class of cell surface adhesion receptors. This paper reports the minimum number of ligands required to support morphologically normal cell spreading with focal contact formation, the requirements for a complete adhesive interaction.

Several model experimental systems have been developed to investigate the minimum number of ligand–receptor interactions to support cell adhesion and spreading. A model system developed by Brandley and Schnaar, which consists of RGD-containing peptides covalently grafted to polyacrylamide gels, has been recently used to study integrin-mediated cell adhesion (2) and haptotactic cell migration on linear and exponential gradients of immobilized RGD peptides (3). The later study demonstrated that cell interactions with these substrates were dependent on RGD surface density. Although well-defined gradients were obtained by the methods used in this study, surface concentrations of peptide at any given region of the gradient substrate could only be approximated. Peptides are highly permeable in the polyacrylamide gel base material, and as such, the peptide was not grafted exclusively on the surface of the gel; thus, only concentrations of peptide per gel volume could be quantified and surface concentrations of peptide were estimated from these values by assigning an arbitrary value for the depth of the gel

1. *Abbreviations used in this paper*: FN, fibronectin; FNR, fibronectin receptor; GRGDY, Gly-Arg-Gly-Asp-Tyr; HFF, human foreskin fibroblast; IRM, interference reflection microscopy; LN, laminin; SEM, scanning electron micrograph; VN, vitronectin; VNR, vitronectin receptor.

that was assumed to be accessible to cells from the surface. In the model of the present study a dense substrate was modified exclusively at the surface, allowing precise quantification of peptide surface concentration.

A second model system for studying integrin-mediated cell adhesion was developed by Danilov and Juliano (6) and consisted of a plastic substrate containing adsorbed conjugate proteins of albumin which had been derivatized with short RGD sequences. RGD density was modulated by controlling the number of RGD peptides grafted to the albumin molecules. Studies with this system demonstrated that the efficiency of cell adhesion increased with increasing amounts of RGD peptide conjugated per protein molecule. Although it is possible to determine the number of RGD conjugates bound to the substrate with this system, the number of RGD moieties actually available for cell interaction (i.e., the effective RGD surface density) is difficult to quantify, since an unknown number of RGD groups are masked from cell surface receptors by the protein conjugate itself, i.e., are pointed toward the plastic substrate rather than toward the cells. Alternatively, an unknown number of RGD groups could be conjugated to the albumin in a manner that renders them inaccessible to the cell surface receptors. It is also quite difficult conceptually to permit two or more large adhesion receptor proteins clustering around one albumin molecule to interact with two or more RGD peptides conjugated thereto. Given that albumin is a relatively small globular protein, it seems likely that steric limitations would prevent such multidentate binding. In the model of the present study, all of the surface-bound peptide ligands are immobilized identically and all are available to the cells for receptor-mediated binding.

Singer et al. (25) also observed RGD density-dependent cell attachment on substrates containing synthetic RGD peptides covalently grafted to adsorbed albumin. Other workers have quantified adsorption of cell adhesion proteins and cell adhesion protein fragments to evaluate the effects of ligand density on receptor-mediated cell adhesion (12, 14, 29). These systems did demonstrate RGD density-dependent cell adhesion, but the fraction of adhesion ligands available for cell adhesion receptors could not be determined directly. This is because of uncertainty about the conformation of the adsorbed protein, namely whether it has significantly denatured upon the surface, and about its configuration relative to the surface, namely whether it has adsorbed such that the receptor-binding domain is oriented away from the underlying substrate. The results of the above described studies using RGD–protein conjugates, RGD-grafted polyacrylamide, and cell adhesion proteins and fragments are presented quantitatively in the discussion and are summarized in Table II associated with that discussion.

The adhesive substrates used in this study are well defined, since the peptides are covalently grafted to the substrate in a single conformation. The peptide is immobilized to an otherwise poorly adhesive glass substrate by the NH_2-terminal amine via a glycyl residue used as a spacer; the COOH-terminal tyrosyl residue is provided for radioiodination. It has been previously shown with radiolabeled peptide accumulation on the substrate (20) that peptide surface concentrations can be precisely measured and controlled, permitting the direct correlation of RGD surface density to the state of cell adhesion and spreading. It was also demonstrated (20) that adsorbing proteins from serum or albumin in the medium, and from cellular sources play only a minimal role in either blocking or promoting the cell adhesive interactions; this is likely because of the poor protein-adsorbing properties of the base glass substrate. As such, the cellular behavior is directly influenced by the quantity and the nature of the surface-immobilized peptide, without the complex conformation issues associated with protein adsorption. We have also recently demonstrated that the peptides so immobilized are resistant to cellular proteolysis for periods of at least 12 wk, and that the adhesive activity is retained after steam autoclaving (Persad and Hubbell, unpublished observations using radiolabeled peptides and adhesion bioassays).

This study investigates the effect of RGD density on cell adhesion and spreading as indicated by the extent of cell spreading, focal contact formation, and cytoskeleton organization. The role of the VN receptor, or integrin $\alpha_v\beta_3$, and the fibronectin receptor, or integrin $\alpha_5\beta_1$, in cell attachment and spreading on these adhesion peptide-derivatized substrates was also examined.

Materials and Methods

Cell Culture

Human foreskin fibroblasts (HFF) were established in culture from neonatal foreskins. Low passage HFFs were maintained in DMEM (Gibco BRL, Gaithersburg, MD) supplemented with 10% FCS (Gibco BRL), 400 U/ml penicillin (Gibco BRL), and 400 μg/ml streptomycin (Gibco BRL) and were incubated at 37°C in a humidified 5% CO_2 atmosphere.

Preparation of Substrates

A three-step chemical process was used for substrate preparation (20). In the first step, glass was rendered relatively poorly cell adhesive by modification with a silylating agent to produce what is called glycophase glass. In the second step, the glycophase glass was activated with sulfonyl chlorides, and in the final step, the activated glycophase glass was coupled to the peptide via the NH_2-terminal primary amine. We have previously shown that under these conditions, all of the peptide added to the activated glycophase glass substrates was immobilized upon the substrate. The amount of immobilized peptide may be accurately controlled by adding the appropriate amount of peptide to the activated glass. Specifically, glass coverslips (18 × 18 mm; Thomas Scientific, Philadelphia, PA) were soaked in 0.5 M sodium hydroxide for 2 h, rinsed in deionized water, and immersed in an aqueous solution (1%, pH 5.5) of (3-glycidoxypropyl)-trimethoxysilane (Hüls America, Inc., Piscataway, NJ). The preparation was heated and maintained at 90°C for 2 h. The coverslips were then washed to remove unreacted silane. 1 mM HCl was added to the dish containing the sialylated glass coverslips and this preparation was heated at 90°C for 1 h to convert the oxirane moieties on the derivatized glass to glycol groups (glycophase glass). Dry glycophase glass coverslips were rinsed with dry dioxane (dried over molecular sieve 4A; Fisher Scientific Co., Pittsburgh, PA). To 10 ml of dry dioxane, 200 μl of dry pyridine and 100 μl of dry tresyl chloride (2,2,2-trifluoroethanesulfonyl chloride; Fluka AG, Buchs, Switzerland) were added. A minimal volume of this mixture was added to the upper surface of each glycophase glass coverslip placed in a glass Petri dish. The reaction was allowed to proceed for 10 min at room temperature, after which the coverslips were rinsed in 1 mM hydrochloric acid and finally rinsed in 0.2 M sodium bicarbonate buffer at pH 10 (coupling buffer). Coupling buffer containing varying Gly-Arg-Gly-Asp-Tyr (GRGDY; Biosynthesis, Inc., Dexton, TX) concentrations was added at a minimal volume on the coverslips and incubated for 20 h at room temperature to graft the peptide to the surface. The buffer was removed after the 20-h incubation period and replaced with coupling buffer containing 0.8 M β-mercaptoethanol, which effectively replaces unreacted tresyl groups. The β-mercaptoethanol was incubated with the coverslips for 2 h so that unreacted tresyl groups would react with a nonadhesive moiety. The peptide was demonstrated to by >95% pure by HPLC by the manufacturer.

Control of Peptide Surface Concentration

Previous studies (20), where radiolabeled GRGDY was coupled to glass by the chemistry outlined above, demonstrated that surface concentrations increased linearly with increasing input levels of GRGDY to a saturated level of grafted peptide (12 pmol/cm^2). The linear relation reported (20) was determined from direct measurements of immobilized radiolabeled GRGDY and the lowest detectable substrate surface concentration of peptide was 2,000 fmol/cm^2. Nearly quantitative immobilization of peptide was achieved over a range of 2,000–12,000 fmol/cm^2 of input peptide. More recently, it was observed that immobilization of GRGDY was nearly quantitative at an input peptide concentration of 30 fmol/cm^2 (S. A. Massia, unpublished results), which suggests that immobilization is quantitative down to this level of peptide surface concentration.

In this report, biological responses were primarily studied with RGD surface concentrations ranging from 0.1 to 100 fmol/cm^2. The various RGD surface densities were obtained by controlling the concentration of peptide in the reaction buffer during the surface immobilization process. Reaction conditions necessary for RGD surface concentrations greater than 30 fmol/cm^2 were interpolated from previous results which demonstrated a linear increase in peptide surface concentration with increasing concentrations of peptide in the reaction buffer up to a surface saturation concentration of 12,000 fmol/cm^2. For RGD surface concentrations below 30 fmol/cm^2, it was assumed that the linear relation between peptide input concentration and immobilized peptide surface concentration extended below the detectable limit of 30 fmol/cm^2. Therefore, input peptide concentrations necessary to obtain RGD surface concentrations below 30 fmol/cm^2 were extrapolated values.

Adhesion Assays

Cells harvested for experiments were rinsed twice with Ca^{2+}- and Mg^{2+}-free PBS and then incubated in 0.54 mM EGTA in PBS for 15 min at 37°C for detachment. Cells were then collected by centrifugation and resuspended in serum-free medium, which consisted of DME with 4 mg/ml of heat-inactivated (90°C for 10 min) BSA (Sigma Chemical Co., St. Louis, MO) and antibiotics. Heat treatment of the albumin achieves the denaturing of contaminating cell adhesion proteins without adversely affecting the albumin (30). The substrates were seeded at a density of 10,000 cells/cm^2 and cells were allowed to attach and spread at 37°C in 5% CO_2. An inverted microscope (Fluovert; Wild Leitz, Inc., Rockleigh, NJ) equipped with phase contrast objectives and a high resolution video camera (67M series; Dage-MTI Inc., Wabash, MI) was used to visualize spreading cells after a 4-h incubation. Random fields of adherent cells were chosen for video recording and at least 100 cells were analyzed on each substrate. Adherent cells were observed and categorized into four morphological types: type I, spheroid with no filapodia; type II, spheroid with one to two filapodia; type III, spheroid with greater than two filapodia; and type IV, flattened and polygonal or flattened with pseudopodia. These morphologies are illustrated in Fig. 1. The population of adherent cells analyzed on each substrate was scored according to the above criteria and the percentage of each morphological type in the sample population was determined for each substrate 4 h after seeding. The percent of attached cells which are spread, as described in (20), was obtained by multiplying the ratio of spread cells to the total number of attached nonspread and spread cells by 100; nonadherent cells were discriminated from adherent ones by gently shaking the dish. Approximately 80% of the cells in each field were adherent and the proportion of nonadherent cells did not appear to vary with peptide density. Focal contacts were observed by interference reflection microscopy as described below without fixation.

Antisera Adhesion-blocking Assays

To identify which class of integrins was involved in promoting attachment and spreading to surface immobilized GRGDY, rabbit polyclonal antisera to the human vitronectin receptor (VNR) and to the human fibronectin receptor (FNR) were used (Telios Pharmaceuticals, San Diego, CA). Anti-human VNR was specific for integrin $\alpha_v\beta_3$ and anti-human FNR was specific for integrin $\alpha_5\beta_1$. A protocol described by Dejana et al. (8) was used for this assay with some modifications. Nonenzymatically harvested cells suspended in serum-free medium were incubated for 30 min before seeding with increasing concentrations of either anti-FNR or VNR separately, or both antibodies combined. In controls, the antibodies were replaced by preimmune rabbit serum (Gibco BRL). As a control for antibody cross reactivity, antiserum-treated cells were incubated on FN- and VN-coated substrates. Cell suspensions preincubated with antibodies or preimmune serum were inoculated on substrates with a RGD surface density of 100 fmol/cm^2 and incubated for 4 h at 37°C. The samples were then washed twice with PBS to remove unattached cells and fixed in 3.7% formaldehyde in PBS for 30 min. The fixed samples were washed and immersed in PBS for phase contrast microscopy. Attached and spread cells were counted in 10 fields at 200× magnification for each sample. Spread cells (type IV morphology) were scored by the criteria of polygonal shape and distinct nuclei. Percent of control cell attachment was determined by dividing the total number of attached spread and nonspread cells for a given experimental condition by the total number of attached spread and nonspread cells observed with preimmune serum-treated cells. This ratio was then multiplied by 100 to obtain the percentage of the control value.

Scanning EM

Samples of adherent cells on the peptide grafted substrates were prepared by fixation with 2% glutaraldehyde in PBS for 1 h. The samples were rinsed in water and dehydrated in a graded ethanol series with 10-min exchanges in each of 25, 50, 75, 95, and 100% ethanol. The samples were dried by sublimation using Pelldri II (Ted Pella Inc., Irvine, CA) according to the manufacturer's directions and sputter coated after mounting on stubs. The specimens were examined in a SEM (model 515; Philips Electronic Instruments, Inc., Mahway, NJ) and photomicrographs were made using P/N film (type 55; Polaroid Corp., Cambridge, MA).

Light Microscopy

For focal contact visualization, cells adherent to peptide-grafted 24 × 50-mm glass coverslips (Thomas Scientific) were mounted in a culture chamber stage and fitted onto an inverted stage microscope (Fluovert; Wild Leitz, Inc.). A NPL Fluotar 100× objective (Wild Leitz, Inc.) was used so that transmission phase contrast and interference reflection microscopy (IRM) (5, 17) could be performed on the same field without changing objectives. Phase contrast and IRM images were acquired from live cells immersed in serum-free medium and maintained at 37°C. Illumination for phase contrast was provided by a 100 W halogen lamp equipped with a heat-reflecting filter and a 100 W mercury lamp was used for IRM. Images were acquired with a high resolution video camera (70 series; Dage-MTI) and digitized with an image processing system (hardware from Image Technology Inc., Woodburn, MA, and software from G. W. Hannaway and Associates, Boulder, CO). Digitized images were photographed after digital contrast enhancement from a high resolution video monitor (model PVM 1271Q; Sony) using Ilford Pan F film. 50 to 100 cells were analyzed for substrates ranging in RGD surface concentrations from 10^{-3} to 10^4 fmol/cm^2 to determine the extent of focal contact formation on each substrate.

To evaluate microfilament networks in spread cells after a 4-h incubation on peptide-grafted glass coverslips, samples were rinsed in PBS and fixed for 20 min with 3.7% formaldehyde in PBS. They were then rinsed in PBS and permeabilized by incubation at room temperature for 1 min in PBS containing 0.2% (vol/vol) Triton X-100 (Sigma Chemical Co.). Cells were then rinsed in PBS and F-actin was stained by incubating for 20 min at room temperature with 900 ng/ml rhodamine-conjugated phalloidin (Molecular Probes Inc., Junction City, OR). The coverslips were rinsed thoroughly with PBS and mounted on microscope slides in 50% PBS–50% glycerol. These preparations were viewed on a Fluovert microscope equipped with a 100× PL Fluotar objective and photographed from the high resolution video monitor after digital contrast enhancement of the video image.

Double-label immunofluorescence was performed to observe the distribution of FNR and VNR in spread cells on the peptide-grafted substrates. The primary antibodies used in these studies, polyclonal rabbit anti-human VNR and monoclonal mouse anti-human α_5, were obtained from Telios Pharmaceuticals, Inc. The secondary antibodies used were FITC-conjugated sheep anti-mouse IgG and cross-species adsorbed TRITC-conjugated donkey anti-rabbit IgG (both from Accurate Chemical and Scientific Corp., Westbury, NY). At various incubation periods, cells on derivatized glass coverslips were rinsed with PBS, fixed in 3.7% formaldehyde (prepared fresh from paraformaldehyde) for 5 min and then permeabilized with Triton X-100 in PBS for 6 min. The samples were then briefly rinsed in PBS and washed in 2 mg/ml BSA in PBS (BSA–PBS) for 5 min. Samples were incubated with a mixture of primary antibodies (diluted 1:10 in BSA–PBS) for 45 min at 37°C. After the first incubation, samples were washed twice in BSA–PBS for 5 min each wash. The samples were then incubated in a mixture of the fluorescent secondary antibodies (diluted 1:50 in BSA–PBS) for 45 min at 37°C. After two 5 min washes in BSA–PBS, the samples were mounted on glass slides with 1:1 glycerol/PBS and sealed with nail polish. Cells adherent to VN- and FN-coated glass substrates were stained using

this double-label protocol to demonstrate positive staining of VNR and FNR. Focal contacts in these samples were visualized via IRM to demonstrate localization of receptors into focal contacts. These preparations were viewed on a Fluovert microscope equipped with a 100× PL Fluotar objective and photographed from the high resolution video monitor after digital contrast enhancement of the video image.

Results

HFF Spreading as a Function of RGD Surface Density

A variety of adherent cell morphologies were observed on the substrates and were categorized into four types as described in the Materials and Methods section. Scanning EM (SEM) micrographs show representative morphologies of each category (Fig. 1). Cell adhesion in serum-free medium was observed on substrates with a RGD surface density of 10^{-3} fmol/cm^2 and 81 ± 3% of the adherent cells analyzed were types I and II morphologies; only 5 ± 0.5% were type IV after a 4-h incubation (Fig. 2). At 10^{-2} fmol/cm^2 of grafted GRGDY, 22 ± 1% of the adherent cells were type IV. Further logarithmic increases in RGD surface concentration resulted in significant increases (by *t* test comparing one condition with the value for the next decade lower concentration; $p<0.005$ for all cases) in the percentage of type IV adherent cells up to, but not beyond, 1 fmol/cm^2 (Fig. 2). SEM revealed that many of the adherent cells were spherical on substrates containing 0.1 fmol/cm^2 of grafted GRGDY (Fig. 3 *A*) whereas adherent cells on substrates above this surface concentration, 1 fmol/cm^2 and greater, displayed predominantly flattened morphologies (Figs. 3, *B–D*).

RGD Density-dependent Focal Contact and Stress Fiber Formation

Cells were examined live by IRM and phase contrast microscopy 4 h after seeding on substrates with RGD surface con-

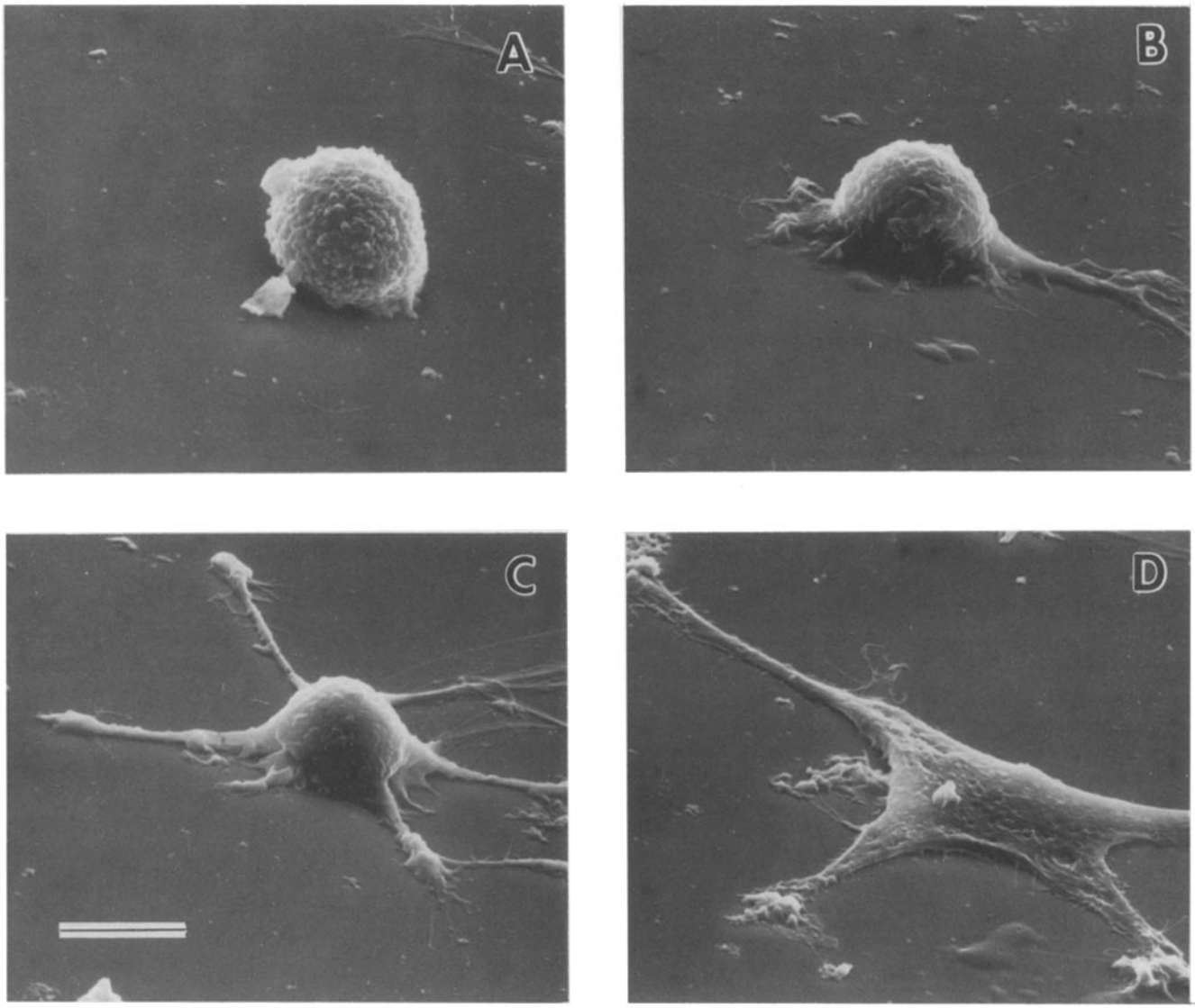

Figure 1. SEMs of adherent cells on substrates containing covalently grafted GRGDY indicating the classification into types I–IV. Cells adherent on substrates with varying surface concentration of peptide were scored according to the four morphological types represented here. (*A*) type I, spheroid cells with no filapodial extensions; (*B*) type II, spheroid cells with one to two filapodial extensions; (*C*) type III, spheroid cells with greater than two filapodial extensions; (*D*) type IV, flattened morphology representative of well spread cells. Bar, 10 μm.

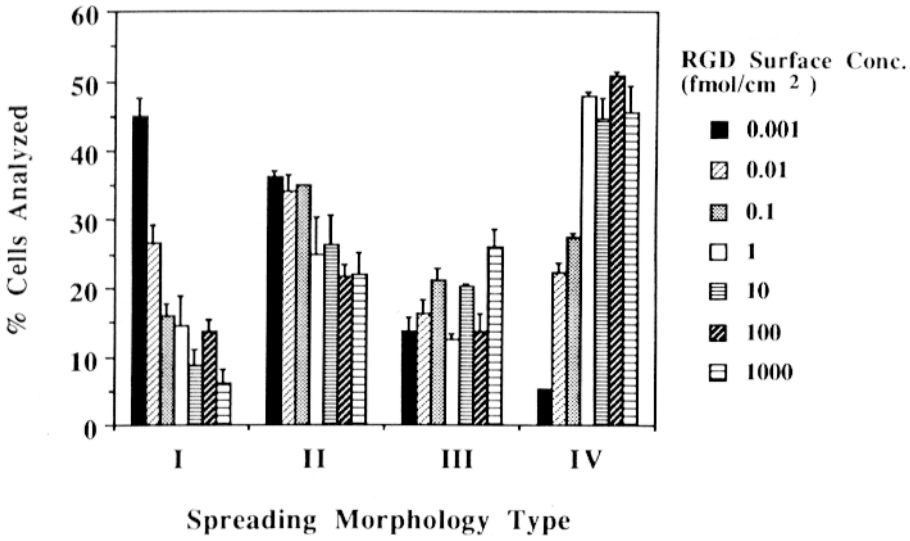

Figure 2. The effects of RGD density on cell spreading. HFFs were suspended in serum-free medium with albumin and incubated on substrates for 4 h. Cells were scored by morphological types which represent the extent of cell spreading and the percentage of each type was determined for each RGD surface density. Samples in individual experiments were run in triplicate, averaged, and mean values were determined from averaged values of three separate experiments; for each sample, at least 100 cells were analyzed. Error bars represent standard error of the mean values. The percentage of cells having type IV morphology increased with increasing RGD surface densities up to 1 fmol/cm^2; $p < 0.005$ for each case compared with the next lowest decade. Further increases in RGD surface density above this value resulted in no significant increases in the combined percentages of type III and IV morphologies. This suggests that 1 fmol/cm^2 is the minimal concentration necessary for complete cell adhesion and spreading.

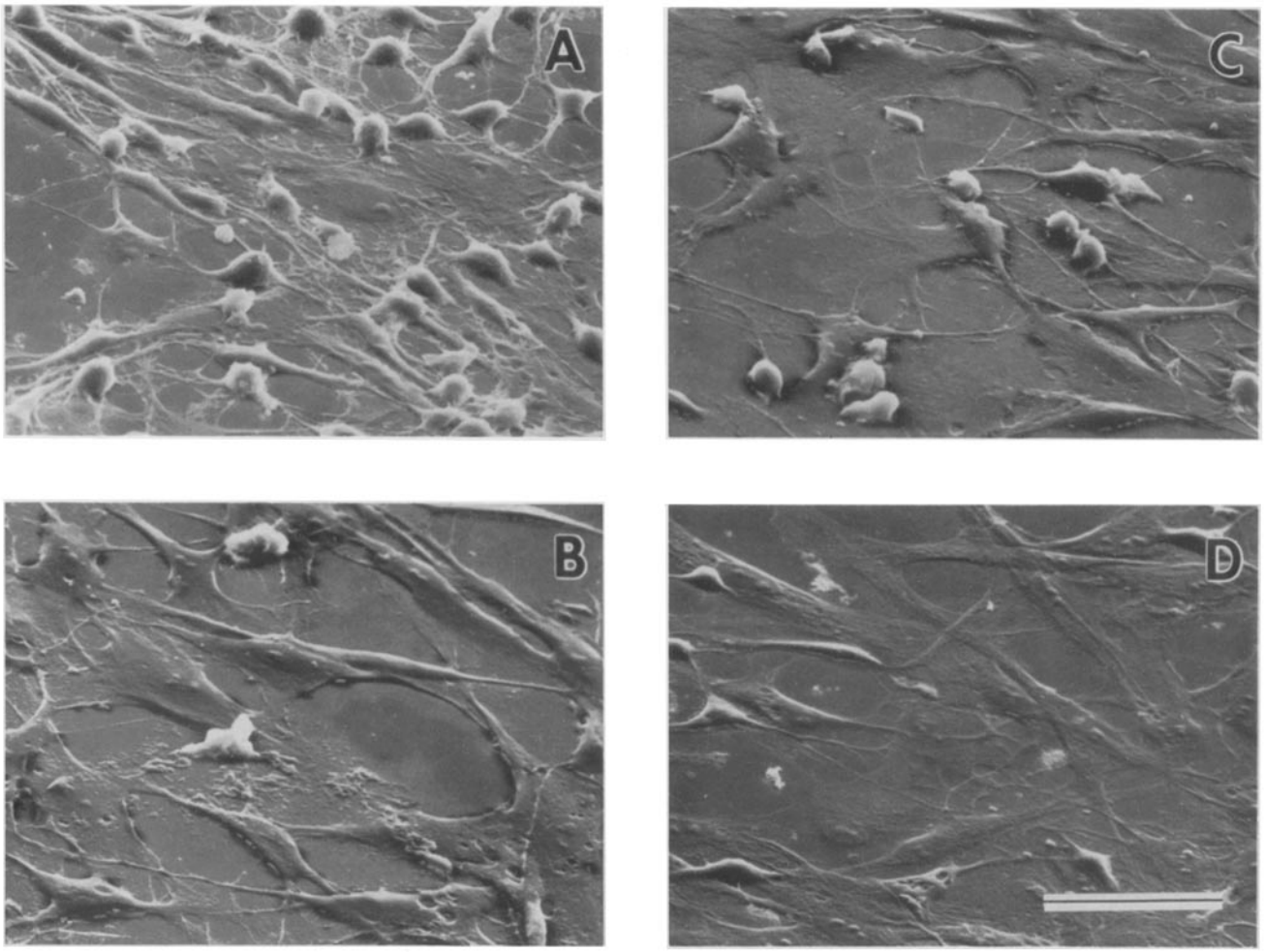

Figure 3. SEMs of cells adherent to substrates with RGD surface densities: 0.1 fmol/cm^2 (*A*), 1 fmol/cm^2 (*B*), 10 fmol/cm^2 (*C*), and 100 fmol/cm^2 (*D*). At 0.1 fmol/cm^2 (*A*), many adherent cells are spherically shaped; most of the adherent cells are well spread at concentrations above this value. Bar, 50 μm.

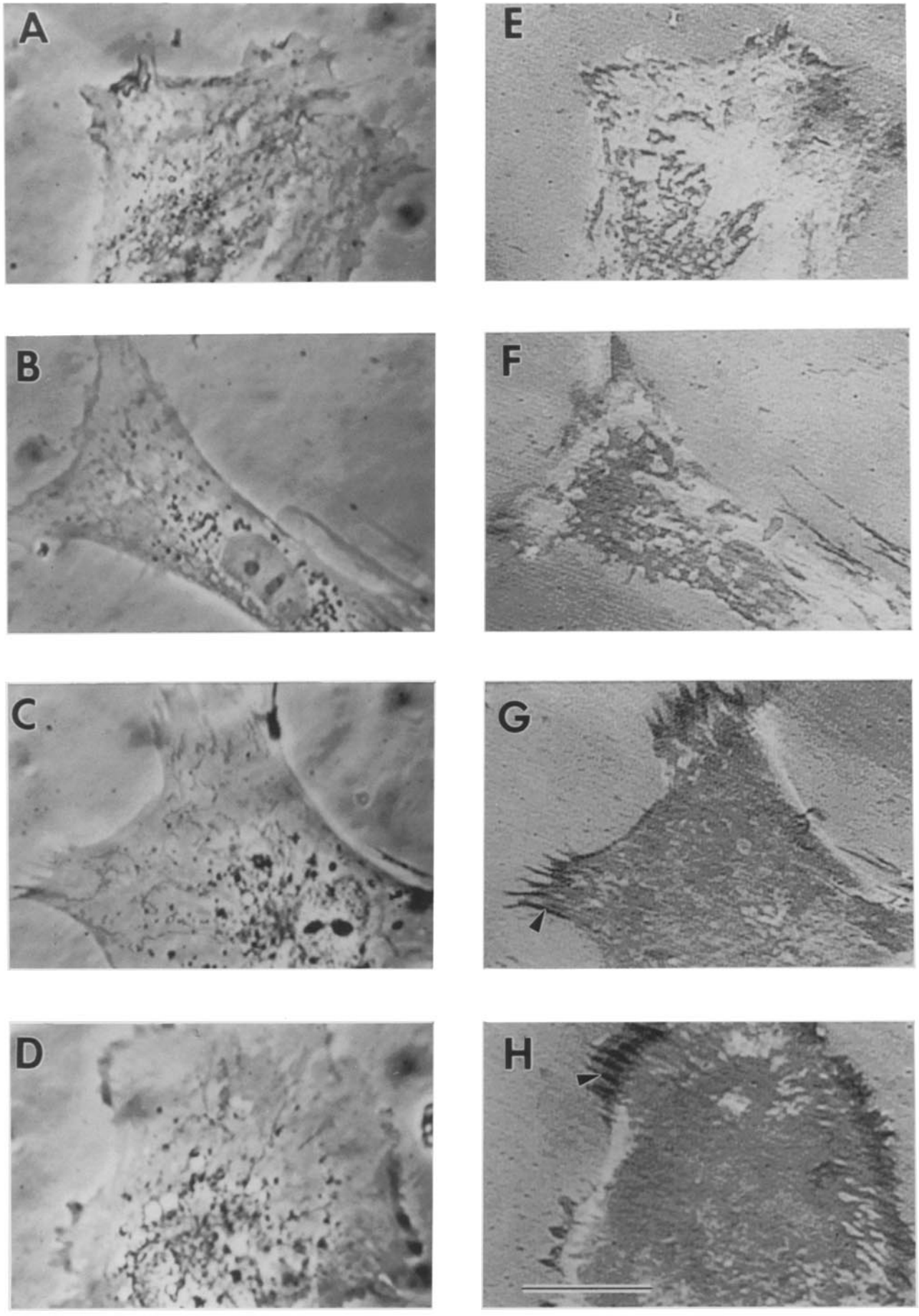
A
B
C
D
E
F
G
H

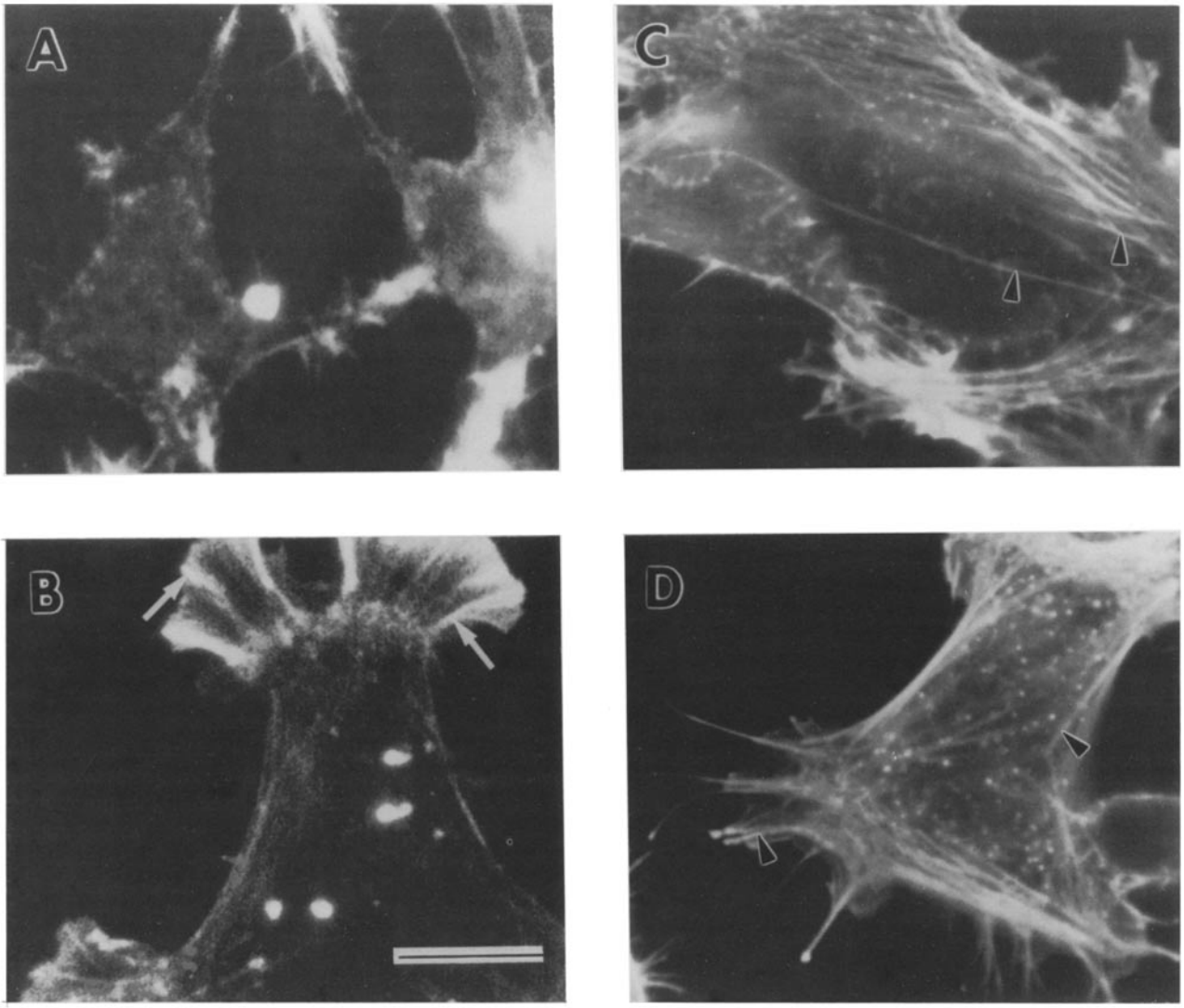

Figure 5. Fluorescence micrographs of well-spread HFFs stained for F-actin by rhodamine-conjugated phalloidin after 4-h incubation. RGD surface concentrations were 0.1 fmol/cm² (*A*), 1 fmol/cm² (*B*), 10 fmol/cm² (*C*), and 100 fmol/cm² (*D*). Cytoskeletal organization was weak in spread cells on substrate surfaces containing 0.1 fmol/cm² (*A*). At 1 fmol/cm², only short thick actin filaments (*arrows*) formed in spread cells (*B*). RGD surface concentrations of 10 and 100 fmol/cm² supported stress fiber formation (*arrowheads*) in spread cells (*C* and *D*). Bar, 20 μm.

centrations ranging from 10^{-1} to 10^{2} fmol/cm². HFFs which were determined to be fully spread by phase contrast microscopy on each substrate (Figs. 4, *A–D*) were analyzed by IRM to visualize focal contacts (Figs. 4, *E–H*). Spreading was maximal on substrates having RGD surface concentrations as low as 1 fmol/cm², but focal contact formation was not prevalent until the surface concentration reached 10 pmol/cm². Spread cells on substrates with surface concentrations below 1 fmol/cm² formed close contacts but not focal contacts as indicated by IRM (Figs. 4, *E* and *F*). At 10 and 100 fmol/cm², focal contacts formed on morphologically well spread cells (Figs. 4, *G* and *H*). It was observed that no focal contacts formed in spread cells when the RGD surface concentration was 10^{-1} fmol/cm² or lower, and at 1 fmol/cm² only 20% of the spread cells had focal contacts. All spread cells analyzed on substrates with the RGD density at 10 fmol/cm² and above were observed to have focal contacts; the critical RGD surface density for focal contact formation was between 1 and 10 fmol/cm² for HFFs.

Rhodamine-conjugated phalloidin staining of spread cells after a 4-h incubation on peptide-grafted substrates revealed extensive actin microfilament formation when the RGD surface concentration was 10 fmol/cm² and above (Figs. 5, *C* and *D*). At 1 fmol/cm², short, thick fibers, which are not

Figure 4. Phase contrast (*A–D*) and interference reflection microscopy (*E–H*) of well-spread cells on RGD-grafted substrates 4 h after inoculation. RGD surface concentrations were 0.1 fmol/cm² (*A* and *E*), 1 fmol/cm² (*B* and *F*), 10 fmol/cm² (*C* and *G*), and 100 fmol/cm² (*D* and *H*). Only close contacts (*dark grey regions*) were apparent in cells spread on substrates with the RGD surface density below 10 fmol/cm² (*E* and *F*). Focal contacts (*arrowheads*) formed in cells when the RGD density was 10 fmol/cm² and above (*G* and *H*). Bar, 20 μm.

characteristic of typical stress fibers in fully spread cells, formed in the periphery of spread cells with poorly formed filaments within the cell body (Fig. 5 *B*). At 10^{-1} fmol/cm², no stress fibers or short fibers were present in spread cells (Fig. 5 *A*).

Effects of FNR and VNR Antisera on HFF Adhesion and Spreading

The role of FNR and VNR in cell attachment and spreading on substrates containing 100 fmol/cm² of surface-grafted GRGDY was investigated by incubating HFFs with antiserum directed against FNR or VNR. Control studies demonstrated that the presence of anti-VNR in the culture medium at a 1:50 dilution completely inhibited HFF attachment and spreading on VN-coated substrates, but not on FN-coated substrates. It was also demonstrated that a 50-fold dilution of anti-FNR in the culture medium completely inhibited attachment and spreading on FN-coated substrates, but not on VN-coated substrates. Furthermore, if both antisera were present at a 50-fold dilution, attachment and spreading was completely inhibited on either the FN- or the VN-coated substrates (control results are summarized in Table I). Anti-VNR blocked adhesion and spreading of HFFs to GRGDY-grafted substrates in a concentration-dependent manner (Fig. 6). Anti-FNR was ineffective in blocking adhesion and spreading to GRGDY-grafted substrates, even at concentrations that completely blocked adhesion and spreading to FN-coated substrates (Fig. 6).

RGD Density-dependent Localization of VNR and Association with Focal Contacts

Double-label immunofluorescence visualization of VNR, FNR, and IRM was used to observe the distribution of VNR and FNR in spread HFFs. HFFs, seeded on peptide-grafted substrates and cultured for 4 h in serum-free medium, spread without focal contact formation at RGD densities of 0.1 and 1 fmol/cm² and formed focal contacts at 10 fmol/cm² of surface-bound GRGDY (Figs. 7, *D–F*; IRM images). Double-label immunofluorescence staining, after a 4-h incubation, revealed no localization of FNRs in spread cells on all peptide-grafted substrates, since a diffuse homogeneous or granular staining pattern was observed in all samples (data not shown). Localization of FNRs in spread cells on FN-coated substrates were demonstrated using this dual-label protocol (data not shown). After a 4-h incubation, diffuse immunofluorescence staining patterns indicated no localization of FNRs on all peptide-grafted substrates (data not shown). IRM revealed focal contacts only in spread cells on substrates containing 10 fmol/cm² of surface-bound GRGDY (Figs. 7, *D–F*). Immunofluorescence staining of VNR, 4 h after seeding, revealed some localization of these receptors in peripheral regions of spread cells on substrates containing 0.1 or 1 fmol/cm² of surface-immobilized GRGDY (Figs. 7, *A* and *B*). At 10 fmol/cm² of surface-bound GRGDY, clustering of VNRs was observed in intensely stained regions which generally colocalized with elongated, mature focal contacts of the field-matched IRM image (Figs. 7, *C* and *F*).

Table I. Inhibition of Cell Attachment and Spreading of HFFs to FNA and VN by Anti-VNR and Anti-FNR Antisera

Antiserum	Substrate*	Percent control attachment	Percent spreading
Preimmune rabbit serum	FN	100	93 ± 2‡
	VN	100	92 ± 2
Anti-VNR	FN	87 ± 7‡	91 ± 4
	VN	14 ± 2	0
Anti-FNR	FN	16 ± 5	14 ± 8
	VN	89 ± 7	93 ± 5
Anti-FNR + Anti-VNR	FN	12 ± 3	15 ± 2
	VN	16 ± 4	0

* Substrates were prepared by adsorbing 20 μg/ml of FN or VN on etched glass coverslips for 1 h followed by adsorption of 1 mg/ml of BSA for 30 min.
‡ Data are mean values from triplicate determinations, with at least 100 cells per determination, ± SEM.

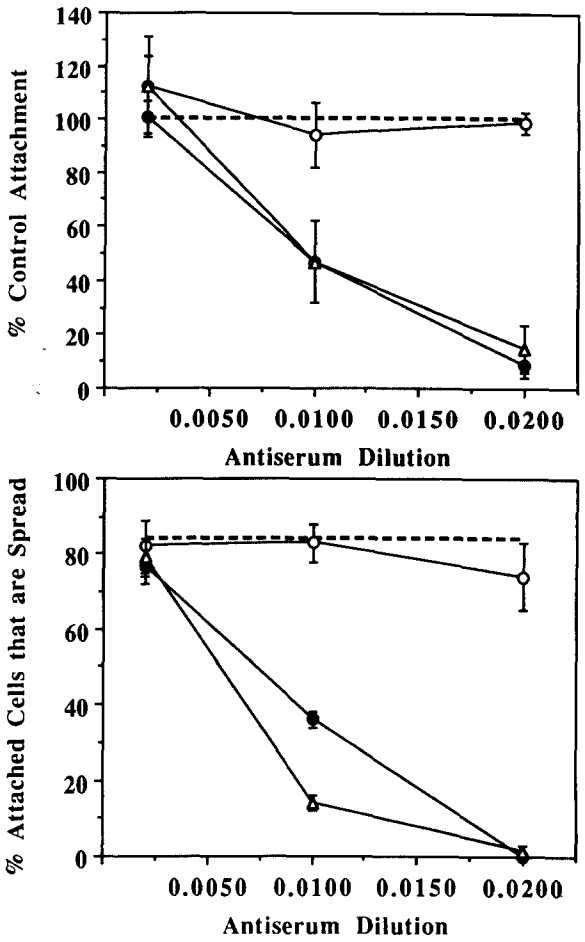

Figure 6. Effects of anti-human VNR and anti-human FNR on HFF attachment and spreading to 100 fmol/cm² of covalently grafted GRGDY. The cells were incubated 30 min before seeding on substrates. The cells were allowed to attach to substrates for 4 h in the presence of antisera or control preimmune serum. Nonadherent cells were removed by washing and the samples were fixed with 3.7% formaldehyde in PBS for 30 min. Adherent cells were viewed and counted by phase contrast microscopy and scored as spread (*type IV* in Fig. 1) or nonspread (*types I–III* in Fig. 1). Control attachment was defined as the number of cells that attached when incubated in the presence of preimmune serum. Control serum (- - -); anti-VNR (●); anti-FNR (○); anti-VNR + anti-FNR (△). Data points are mean values from triplicate determinations, with at least 100 cells in each determination; error bars represent standard error of the mean values.

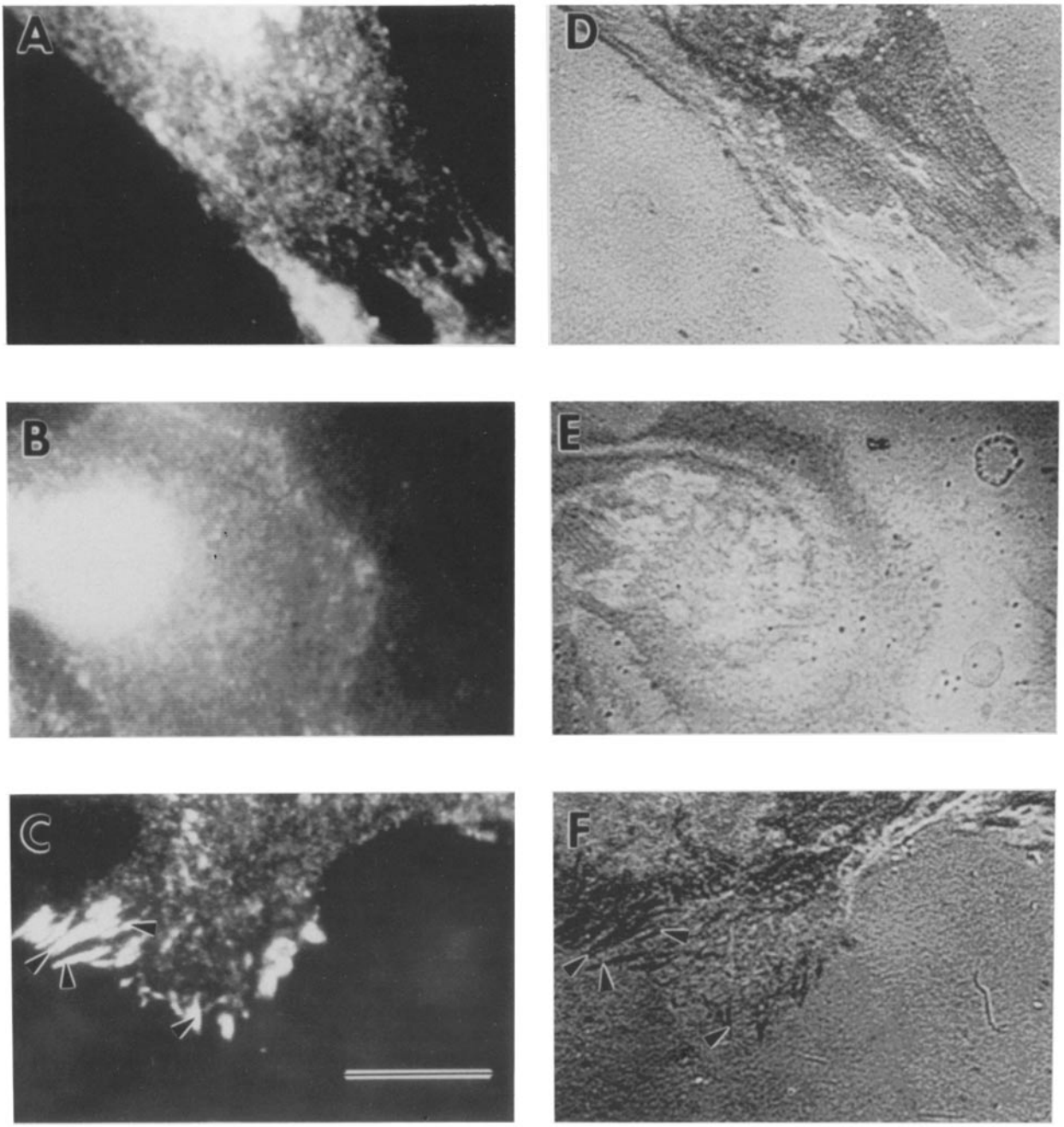

Figure 7. Double-label immunofluorescence (*A–C*) and interference reflection microscopy (*D–F*) of well-spread cells on RGD-grafted substrates 4 h after inoculation. RGD surface concentrations were 0.1 fmol/cm² (*A* and *D*), 1 fmol/cm² (*B* and *E*), and 10 fmol/cm² (*C* and *F*). No focal contacts formed in spread cells on substrates with an RGD surface density below 10 fmol/cm² (*A* and *B*). Furthermore, staining for VNR was generally uniform, which indicated no clustering of these receptors (*D* and *E*). Larger more mature focal contacts (*arrowheads*), which were generally 5 μm in length or greater, were present in spread cells when the RGD density was 10 fmol/cm² (*C*). Intense staining for VNR was noted generally in focal contacts (*arrowheads*), which indicated VNR clustering in these regions (*F*). No clustering of FNR was observed. Bar, 20 μm.

Discussion

In previous studies it was demonstrated that adhesion-promoting peptide sequences covalently grafted to the surface of glycophase glass promoted HFF adhesion and spreading. Furthermore it was demonstrated that the surface density of RGD could be precisely controlled by the quantity of peptide added to the coupling buffer (20). In this report, we use these adhesion peptide-grafted substrates to examine the effects of RGD surface density on integrin-mediated cell adhesion and spreading, and quantify the minimal surface density necessary for maximal cell spreading and the appearance of focal contacts. Complete spreading was observed at a minimal RGD density of 1 fmol/cm² (Fig. 2). At this level, however, focal contacts were observed in only 20% of the fully spread cells examined. Additionally, well established stress fibers were not observed (Fig. 5 *B*). At a level

Table II. Comparison of Results Using Various Experimental Models

Reference	Minimal amount required for spreading or focal contacts					To obtain
	Protein or conjugate	Spacing	Ligand/μm^2	fmol/cm^2	Ligand/Cell*	
		nm				
Humphries et al. (14)	Fibronectin fragment containing RGDS	10	12,000	2,000	2.4×10^7	Spreading
	Fibronectin	12	7,800	1,300	1.6×10^7	Spreading
Singer et al. (25)	RGD-albumin	16	4,500	750	9×10^6	Attachment
Underwood et al. (29)	Vitronectin	20	2,700	450	5.5×10^6	Spreading
	Fibronectin	37	840	140	1.7×10^6	Spreading
Danilov et al. (6)	RGD-albumin	22	2,400	400	4.8×10^6	Spreading
	Vitronectin	22	2,400	400	4.8×10^6	Spreading
	Fibronectin	42	650	110	1.3×10^6	Spreading
Brandley et al. (2)	RGD-Polyacrylamide	76‡	200	33	4×10^5	Spreading
Hughes et al. (12)	Fibronectin	80	180	30	3.6×10^5	Spreading
This study	RGD-Glass	440	6	1	1.2×10^4	Spreading
	RGD-Glass	140	60	10	1.2×10^5	Focal contacts and stress fibers

* Based on a spread cell area of 2,000 μm^2 (20).
‡ All values based on the arbitrary choice of the top 10 nm of the gel being accessible to the cell for ligand binding.

of 10 fmol/cm^2, focal contacts (Fig. 4 *G*) and well-organized stress fibers (Fig. 5 *C*) were apparent in all of the cells observed. The value of 1 fmol/cm^2 required for maximal spreading corresponds to six ligands/μm^2, ~12,000 ligands/spread cell (assuming a characteristic spread-cell area of 2,000 μm^2/cell; 20), or an average peptide-to-peptide spacing of 440 nm. The value of 10 fmol/cm^2 required for maximal spreading, focal contact formation, and stress fibers corresponds to 60 ligands/μm^2, ~120,000 ligands/spread cell, or an average peptide-to-peptide spacing of 140 nm. Interestingly at the 4-h time point roughly 30% of the cells remain in an unspread type I or II morphology at even high peptide surface densities (Fig. 2); it was not determined whether these cells will spread given more contact time.

The surface concentrations required for cell attachment as determined by this study, where all peptides are identically immobilized and available to the cells, are considerably below the values determined in previous studies. A comparative analysis is shown in Table II. Danilov and Juliano (6) addressed this problem using albumin-RGD conjugates adsorbed to tissue culture plastic substrates. They estimated a characteristic peptide-to-peptide spacing required for full attachment of 22 nm, corresponding to 2,400 ligands/μm^2 or 400 fmol/cm^2. Singer et al. (25) used a similar system where albumin was adsorbed and then conjugated with quantifiable amounts of RGD-containing peptides. Their minimal spacing requirement was estimated to be 16 nm, corresponding to 4,500/μm^2 or 750 fmol/cm^2. These RGD surface concentration values are 40 and 75 times in excess of that obtained in this study, suggesting that only a small fraction of the RGD peptide in the albumin conjugates are sterically recognizable or available to the cells. This could be caused by linking of the RGD ligand in the albumin conjugate in a location or configuration not accessible to the receptor. Additionally, for the model adhesion substrate of Danilov and Juliano (6), the peptide ligand was conjugated to all sides of the albumin carrier protein, so some fraction of the ligand (at least half) is shielded from the cell by the carrier protein. Moreover, in the study by Danilov and Juliano (6), up to 20 RGD peptides were linked per albumin molecule. It is clear that only a small fraction of these peptides are available to the cell, since the receptors cannot crowd that closely together.

Brandley and Schnaar (2) addressed the issue of the minimal ligand density by covalently incorporating an RGD-containing nonapeptide into a polyacrylamide gel. The peptide was incorporated throughout the gel, and as such quantitation of the ligand concentration actually at the surface, available to the cells, is quite difficult. Based on the authors' assumption that peptide in the outer 10 nm of the gel is accessible to cells, a peptide-to-peptide spacing of 76 nm is obtained, corresponding to 200 ligands/μm^2 or 33 fmol/cm^2. This surface concentration is threefold in excess of the results in the present study.

Studies with adsorbed whole proteins have also yielded required surface concentrations considerably greater than this study. Danilov and Juliano (6) adsorbed FN and VN to tissue culture plastic surfaces and examined cell attachment as a function of adsorbed protein surface concentration. Their studies indicated a required RGD-to-RGD distance of <22 nm for VN and 42 nm for FN, each of which is less than the values of 140 and 440 nm obtained in this work for complete spreading with and without focal contacts, respectively. Studies by Humphries et al. (14) with adsorbed FN or a FN cell-binding fragment required a minimum RGD spacing of 10 nm for maximum spreading on FN and a minimum spacing of 12 nm for the cell-binding fragment. This suggests that many of the proteins may be adsorbed in an orientation in which the cell-binding domain is inaccessible to the cell, or that the three-dimensional conformation of the protein is sufficiently altered by adsorption to greatly reduce its affinity for the adhesion receptor. Such surface adsorption-induced denaturation, with corresponding loss of affinity for its receptors, has been demonstrated for fibrinogen and its blood platelet surface receptor glycoprotein IIb/IIIa (19).

Similar studies with adsorbed whole adhesion proteins have also been performed with FN and VN by Underwood and Bennet (29). Although not presented in this format, their data with BHK-21 cells can be used to show that they obtained 75% maximal adhesion on VN at a ligand-to-ligand

spacing of 20 nm, corresponding to 450 fmol/cm². The result on FN was 37 nm, corresponding to 140 fmol/cm². Comparison of these results with the results reported here suggests, as described above, that only a small fraction of the adsorbed protein was conformationally available to the cell surface adhesion receptors.

Hughes et al. (12) quantified FN adsorption on substrates and estimated the minimal spacing requirement for maximal spreading at 80 nm, corresponding to 30 fmol/cm². This value is in reasonable agreement with the value of 10 fmol/cm² obtained in the present study. However, overestimation of the spacing requirement was possibly due to the assumption that all cell-binding domains in the adsorbed FN molecules were accessible to cell adhesion receptors.

Many investigators have examined the relative roles of mammalian FNR and VNR in cellular adhesion (7, 8, 9, 26), since FN and VN are two dominant serum components that promote the attachment and spreading of cultured cells (11, 16, 28). In this study, we investigated the role of human VNR and FNR in the adhesion and spreading of HFFs to substrates containing covalently grafted GRGDY with antibodies which functionally block human VNR and FNR. When VNR was blocked, HFF attachment and spreading was inhibited; however FNR-blocking antibody had no effect on these activities (Fig. 6), which suggested a dominant role for VNR in promoting cell attachment and spreading to the GRGDY-grafted substrates examined in this particular study. Double-label immunofluorescence microscopy confirmed the role of VNR in cell spreading to these substrates, since clustering and concentration of adhesion receptors into focal contacts was observed exclusively with VNR (Fig. 7). These data suggest that VNR has a higher affinity for GRGDY than FNR, and therefore plays the key role in promoting cell attachment and spreading to this particular surface-immobilized GRGDY peptide.

Other workers have demonstrated fibroblast attachment, spreading, and focal contact formation mediated by substrate-bound RGD peptides. Singer et al. (25) demonstrated that GRGDS-derivatized substrates (adsorbed albumin conjugates) was sufficient for focal contact formation in spread rat (NRK) and hamster (Nil 8) fibroblasts, but not in spread Balb/C 3T3 fibroblasts. Streeter and Rees (27) demonstrated GRGDSC-mediated focal contact formation in spread NRK fibroblasts and noted differences in focal contact morphology of spread cells on FN- and albumin conjugate–coated substrates. Streeter and Rees (27) also observed weak stress fiber formation in spread NRKs on GRGDS substrates. These effects could be because of FNR-mediated removal of adsorbed conjugate proteins, similar to the FNR-mediated removal of substrate-bound FN reported by Grinnell (10). The contractile activity necessary for cell spreading could be strong enough to remove substrate-bound conjugate protein and alter focal contact shape and stress fiber formation. In this report, normal focal contact formation and stress fiber formation was observed in spread cells on substrates containing sufficient surface concentrations of GRGDY (Figs. 4 and 5). These observations could be due to the adhesion ligand being covalently bound to the substrate surface, therefore receptor-mediated removal of adhesion ligands from the substrate surface is difficult and sufficient contractile force could be generated to produce normal focal contacts and extensive stress fiber formation.

Another study by Singer et al. (26) demonstrated an accumulation of FNR and VNR in focal contacts of spread human gingival fibroblasts on adsorbed GRGDS conjugates after a 1-h incubation. This result contradicts our observation of a predominance of VNR in focal contacts (Fig. 7). Studies by Pierschbacher and Ruoslahti (21) demonstrated that the substitution of Y for S in the peptide GRGDSPC did not effect the affinity of that peptide for VNR and had a higher affinity for VNR than FNR. Furthermore, these workers demonstrated that cyclic GRGDSPC (conformational flexibility is restricted in the cyclic form) has an increased affinity for VNR in comparison to the linear form and an extremely low affinity for FNR (21). Since conformational flexibility of GRGDY is somewhat restricted by the covalent attachment of the NH_2-terminal G to the substrates used in this study, and GRGDY binds to VNR with a higher affinity than that of FNR, it is reasonable to assume that covalently bound GRGDY is a more favorable substrate for VNR binding than for FNR binding. Therefore HFF attachment and spreading would be dominated by VNR on these substrates containing covalently grafted GRGDY, as observed in this study.

The present study has more precisely determined the minimum RGD surface concentration necessary for maximal cell spreading, 1 fmol/cm² or a peptide-to-peptide spacing of 440 nm. Focal contact and stress fiber formation in spread HFFs could be promoted singly by the RGD ligand at a surface concentration tenfold greater than that necessary for maximal spreading, 10 fmol/cm², or a spacing of 140 nm. The VN receptor ($\alpha_v\beta_3$) was demonstrated to be the predominant receptor involved in these interactions on this particular substrate. This model cell adhesion substrate system may be useful in evaluating the cellular response to synthetic peptide domains immobilized at known concentrations and in known conformations.

Special thanks to J. Swanson and G. Arrindell for technical assistance.

This work was supported by grants CBT-8810268 and ECS-8915178 from the National Science Foundation and by a grant from the Texas Advanced Technology Program.

Received for publication 5 November 1990 and in revised form 5 April 1991.

References

1. Abelda, S. M., and C. A. Buck. 1990. Integrins and other cell adhesion molecules. *FASEB (Fed. Am. Soc. Exp. Biol.) J.* 4:2868–2881.
2. Brandley, B. K., and R. L. Schnaar. 1988. Covalent attachment of an Arg-Gly-Asp sequence peptide to derivatizable polyacrylamide surfaces: support of fibroblast adhesion and long-term growth. *Anal. Biochem.* 172:270–278.
3. Brandley, B. K., and R. L. Schnaar. 1989. Tumor cell haptotaxis on covalently immobilized linear and exponential gradients of a cell adhesion peptide. *Dev. Biol.* 135:74–86.
4. Buck, C., and A. F. Horwitz. 1987. Cell surface receptors for extracellular matrix molecules. *Annu. Rev. Cell Biol.* 3:179–205.
5. Curtis, A. S. G. 1964.The mechanism of adhesion of cells to glass. *J. Cell Biol.* 20:199–215.
6. Danilov, Y. N., and R. L. Juliano. 1989. $(Arg\text{-}Gly\text{-}Asp)_n$-albumin conjugates as a model substratum for integrin-mediated cell adhesion. *Exp. Cell Res.* 182:186–196.
7. Dejana, E., S. Colella, G. Conforti, M. Abbadini, M. Gaboii, and P. C. Marchisio. 1988. Fibronectin and vitronectin regulate the organization of their respective Arg-Gly-Asp receptors in cultured human endothelial cells. *J. Cell Biol.* 107:1215–1223.
8. Dejana, E., M. G. Lampugnami, M. Giorgi, M. Gaboli, A. B. Federici, Z. M. Ruggeri, and P. C. Marchisio. 1989. Von Willebrand factor promotes endothelial cell adhesion via an Arg-Gly-Asp-dependent mechanism. *J. Cell Biol.* 109:367–375.
9. Fath, K. R., C. S. Edgell, and K. Burridge. 1989. The distribution of dis-

tinct integrins in focal contacts is determined by the substratum composition. *J. Cell Sci.* 92:67–75.
10. Grinnell, F. 1986. Focal adhesion sites and the removal of substratum-bound fibronectin. *J. Cell Biol.* 103:2697–2706.
11. Hayman, E. G., M. D. Pierschbacher, S. Suzuki, and E. Ruoslahti. 1985. Vitronectin- a major cell attachment promoting protein in fetal bovine serum. *Exp. Cell Res.* 160:245–258.
12. Hughes, R. C., S. D. J. Pena, J. Clark, and R. R. Dourmashkin. 1979. Molecular requirements for the adhesion and spreading of hamster fibroblasts. *Exp. Cell Res.* 121:307–314.
13. Humphries, M. J. 1990. The molecular basis and specificity of integrin-ligand interactions. *J. Cell Sci.* 97:585–592.
14. Humphries, M. J., S. K. Akiyama, A. Komoriya, K. Olden, and K. M. Yamada. 1986. Identification of an alternatively spliced site in human plasma fibronectin that mediates cell type specific adhesion. *J. Cell Biol.* 103:2637–2647.
15. Hynes, R. O. 1987. Integrins: a family of cell surface receptors. *Cell.* 48:549–554.
16. Hynes, R. O., and K. M. Yamada. 1982. Fibronectins: multifunctional modular glycoproteins. *J. Cell Biol.* 95:369–377.
17. Izzard, C. S., and L. R. Lochner. 1976. Cell-to-substrate contacts in living fibroblasts: an interference reflexion study with an evaluation of the technique. *J. Cell Sci.* 21:129–159.
18. Juliano, R. L. 1987. Membrane receptors for extracellular matrix macromolecules: relationship to cell adhesion and tumor metastasis. *Biochim. Biophys. Acta.* 907:261–278.
19. Lindon, J. L., G. McManama, L. Kushner, E. W. Merrill, and E. W. Salzman. 1986. Does the conformation of adsorbed fibrinogen dictate platelet interactions with artificial surfaces? *Blood.* 68:355–362.
20. Massia, S. P., and J. A. Hubbell. 1990. Covalent surface immobilization of Arg-Gly-Asp- and Tyr-Ile-Gly-Ser-Arg-containing peptides to obtain well-defined cell-adhesive substrates. *Anal. Biochem.* 187:292–301.
21. Pierschbacher, M. D., and E. Ruoslahti. 1987. Influence of stereochemistry of the sequence Arg-Gly-Asp-Xaa on binding specificity in cell adhesion. *J. Biol. Chem.* 262:17294–17298.
22. Ruoslahti, E. 1988. Fibronectin and its receptors. *Annu. Rev. Biochem.* 57:375–413.
23. Ruoslahti, E. 1991. Integrins. *J. Clin. Invest.* 87:1–5.
24. Ruoslahti, E., and M. D. Pierschbacher. 1987. New perspectives in cell adhesion: RGD and integrins. *Science (Wash. DC).* 238:491–497.
25. Singer, I. I., D. W. Kawka, S. Scott, R. A. Mumford, and M. W. Lark. 1987. The fibronectin cell attachment sequence Arg-Gly-Asp-Ser promotes focal contact formation during early fibroblast attachment and spreading. *J. Cell Biol.* 104:573–584.
26. Singer, I. I., S. Scott, D. W. Kawka, D. M. Kazazis, J. Gailit, and E. Ruoslahti. 1988. Cell surface distribution of fibronectin and vitronectin receptors depends on substrate composition and extracellular matrix accumulation. *J. Cell Biol.* 106:2171–2182.
27. Streeter, H. B., and D. A. Rees. 1987. Fibroblast adhesion to RGDS shows novel features compared with fibronectin. *J. Cell Biol.* 105:507–515.
28. Tomasini, B. R., and D. F. Mosher. 1990. Vitronectin. *Prog. Hemost. Thromb.* 10:269–305.
29. Underwood, P. A., and F. A. Bennett. 1989. A comparison of the biological activities of the cell-adhesive proteins vitronectin and fibronectin. *J. Cell Sci.* 93:641–649.
30. Woods, A., J. R. Couchman, S. Johansson, and M. Hook. 1986. Adhesion and cytoskeletal organization of fibroblasts in response to fibronectin fragments. *EMBO (Eur. Mol. Biol. Organ.) J.* 5:665–670.